

Structure and Properties of 1,4-Bis(Trinitromethyl)Benzene

 Ian D. Giles,^{*,[a]} Gregory H. Imler,^[a] and Jeffrey R. Deschamps^[a]

Abstract: The structure, activation energy, onset temperature, heat of formation, and calculated detonation properties of 1,4-bis(trinitromethyl)benzene are reported here. The crystal structure of this compound shows that as other trinitromethyl containing compounds the planes of the three independent C-NO₂ are approximately perpendicular to one another. The crystal density is 1.805 g/cm³. Like oth-

er trinitromethyl containing explosives, the onset temperature is relatively low (103.7 °C). The incorporation of two trinitromethyl groups yields a reasonable oxygen balance (−25.5 %) which is close to that of RDX (−21.6 %). While the calculated detonation velocity of HNX exceeds that of TNT it is almost 6 % lower than that of RDX.

Keywords: Energetic materials · Activation energy · Oxygen balance

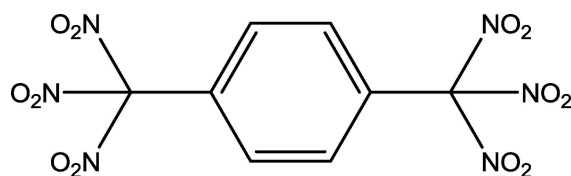
1 Introduction

Designing new explosives requires balancing performance, sensitivity, and cost. Many of the explosives currently in use are the result of low-cost starting materials and synthesis, and acceptable levels of performance.

Higher performance generally results from higher crystal density, higher heat of formation, and higher oxygen balance (which results in the production of carbon dioxide rather than carbon monoxide). Thus materials designed for higher performance typically have a higher oxygen balance. A consequence of this is the incorporation of the trinitromethyl group in an attempt to improve the oxygen balance. Trinitromethyl-based explosives have been known for some time. Based on calculations this class of explosives is likely to be high-energy, dense materials (HEDMs).

Here we report the structure and properties of 1,4-bis(trinitromethyl)benzene (i.e. hexanitro-xylene or HNX), the synthesis of which has been previously reported [1].

unique reflections, and 1068 were observed with $F_o > 3\sigma(F_o)$. The structure was solved and refined with the aid of the SHELXTL system of programs [2]. The full-matrix least-squares refinement varied 124 parameters: atom coordinates and anisotropic thermal parameters for all non-H atoms, and H atoms included using riding model [coordinate shifts of C applied to attached H atoms, C–H distance set to 0.96 Å, H angles idealized, $U_{iso}(H)$ set to 1.1 $U_{eq}(C)$ of, if methyl, 1.2 $U_{eq}(C)$].



1,4-bis(trinitromethyl)benzene (HNX)

2 Experimental Section

2.1 X-Ray Diffraction

A clear colorless 0.42 × 0.52 × 0.55 mm crystal of HNX, in the shape of a prism, was used for data collection on an automated Siemens R3 m/V diffractometer equipped with an incident beam monochromator. Lattice parameters were determined from 25 centered reflections between 30.0° and 34.60° 2θ. The data collection range of hkl was: $0 \leq h \leq 7$, $0 \leq k \leq 10$, $-15 \leq l \leq 15$. Three standards, monitored after every 97 reflections, exhibited random variations with deviations up to ±3.5 % during the data collection. A set of 1499 reflections was collected in the $\theta/2\theta$ scan mode using a variable ω scan rate (a function of count rate) ranging from 7.1 °/min to 14.6 °/min. The dataset contained 1228

2.2 Activation Energy

The thermal activation energy (E_a) of a material's decomposition was measured using the established method of Flynn and Wall [3], initially developed for polymer degradation but applicable to any unimolecular decomposition process such as those measured by ThermoGravimetric Analysis (TGA). TGA runs are performed with approximately equal sample masses. Individual runs collected at different heating rates (see below for the heating rates used for each material) were performed to acquire the data required for determination of E_a . The samples are placed in 100 μL plati-

[a] I. D. Giles, G. H. Imler, J. R. Deschamps
Center for Biomolecular Science and Engineering
U.S. Naval Research Laboratory
Washington, D.C. 20375
*e-mail: ian.giles@nrl.navy.mil

num TGA pans and spread out as much as possible to ensure even heating of the entire sample. By plotting $1/T$ versus $\ln(Ks^{-1})$, the slope of the linear fit, $-E_a/RT$, can be calculated and subsequently solved for E_a . The preexponential factor is estimated using the iterative method of Zsako and Zsako [4].

Heating rates of 1, 2, 3, 4, and 5 °C min⁻¹ were used for all samples. The range of weight percent values used in the determination of the activation energy was determined by establishing the region in which linear fits of each TGA trace for a particular energetic material reached an R^2 of 0.999 to ensure linearity. Temperature values were taken at 0.1% weight loss intervals for each in the ranges specified below:

HNX: 50.0 to 70.0% weight loss.

RDX: 20.0 to 65.0% weight loss.

PETN: 10.0 to 50.0% weight loss.

TATB: 10.0 to 50.0% weight loss.

TNT: Not determined.

2.3 Onset Temperature

Exotherm onset temperatures were measured in a TA Instruments Discovery Series Differential Scanning Calorimeter (DSC) in stainless steel pressure pans sealed with gold-plated copper seals and heated at a rate of 1 °C min⁻¹ to minimize the effects of thermal lag. Each material was measured in quadruplicate and the onset temperatures, as determined using the TA Instruments Trios software, were averaged together and a sample standard deviation calculated.

2.4 Calculated Properties

Detonation velocity and detonation pressure of an energetic material can be calculated from the heat of formation (ΔH_f°), density, and some assumptions on the product distribution on detonation. This is commonly done using CHEETAH [5]. The heat of formation of HNX was calculated by the method of Rice & Byrd [6], density was obtained from the results of the crystallographic study.

3 Results and Discussion

3.1 Crystal Structure

The molecule of HNX sits on a crystallographic center of symmetry located in the center of the 6-membered ring,

such that only half of the atoms in the molecule are independent and have a density of 1.805 g cm⁻³. The results are shown in Figure 1.

The planes of the three independent C-NO₂ groups are approximately perpendicular to one another (interplanar angles are 84.3, 80.4 and 69.8°). Evidence for steric crowding of the three nitro groups on C1a is shown by the long C–N bonds (1.544(3), 1.534(3) and 1.524(3) Å) and close N...O intramolecular approaches (N1 to O2b and N2 to O3b both at 2.54 Å and N3 to O1a at 2.57 Å). Approximately perpendicular planes of the nitro groups and long C-NO₂ bonds are typical of the trinitromethyl group. Based on data in the Cambridge Structural Database (CSD) [7] the average length of a C-NO₂ bond in a trinitromethyl group is 1.526(16) Å as compared to all other the C-NO₂ bonds in the CSD whose average length is 1.481(52) Å. The average angle between the planes formed by the nitro groups is 78.2° in HNX. For all of the entries in the CSD containing a trinitromethyl group, the average plane-plane angle is 77° ± 11°.

Atomic coordinates for HNX are available as Supplementary Information to this article.

3.2 Activation Energy and Onset

The decomposition activation energy of HNX is has been determined to be 400 kJ mol⁻¹. As seen in Table 1, its decomposition activation energy is higher than that of PETN, RDX, and TATB. Despite its higher activation energy, its exo-

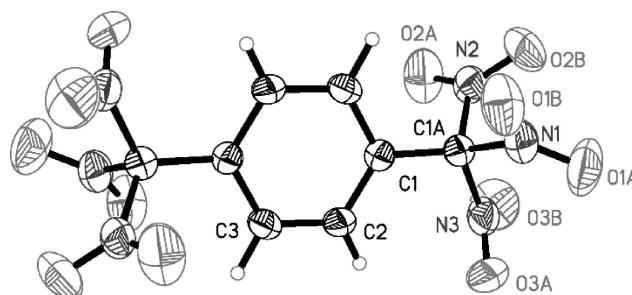


Figure 1. Structure of 1,4-bis(trinitromethyl)benzene as determined by x-ray diffraction. Displacement ellipsoids are at the 50% level. The independent atoms in the asymmetric unit are labeled (unlabeled atoms are symmetry equivalents).

Table 1. Onset temperature and activation energy of HNX and some common energetic materials.

Material	T_{onset} (°C)	E_a (kJ mol ⁻¹)
HNX	103.7 ± 0.8	400 ± 8
RDX	217.9 ± 2.4	289.0 ± 0.2
PETN	171.1 ± 1.3	324 ± 1
TNT	263.5 ± 4.3	Not determined
TATB	334.7 ± 1.1	293 ± 3

Table 2. Heat of formation (ΔH_f , kJ mol⁻¹) calculated using the group additivity method of Rice and Byrd [6] (ΔH_f (calc)) and experimentally determined literature values (ΔH_f (lit.)), detonation velocity (m sec⁻¹), and detonation pressure (GPa) of HNX and some common energetic materials.

Material	ΔH_f (calc)	ΔH_f (lit)	Det V	Det P
HNX	36	73 [8]	8240	30
RDX	86	79 [10]	8875	34
PETN	-515	-540 [11]	8572	31
TNT	-67	-63 [12]	7180	20
TATB	126	-140 [12]	8459	30

therm onset temperature, as measured by DSC, is less than all other energetic materials listed, suggesting limited usage and stability in high-temperature environments. It should be noted that the activation energy of HNX reported here differs from that reported earlier by Yan and Guan, who report an activation energy of 109 kJ mol⁻¹ based on the shift of the heat curve maximum at heating rates of 2, 5, 10, and 20 °C min⁻¹ using differential thermal analysis in open aluminum cups [8]. We suspect this is because of the differing means of detecting reactions changes (heat flow in a DSC or DTA as opposed to mass loss in a TGA) and that the TGA is, at the lower heating rates employed, capturing the activation energy of the initial molecular decomposition events that occur during the induction phase of a DSC exotherm, as discussed by Brill and James [9]. This also likely explains discrepancies regarding the other standard energetic materials to literature values which were also measured using DSC or DTA. More study regarding the clear differences between methods is certainly warranted, but outside the scope of this article.

3.3 Calculated Properties

The heats of formation and detonation properties of HNX and some common explosives are reported in Table 2.

The oxygen balance of HNX is -25.5% with respect to CO₂. For comparison, the oxygen balance of RDX, PETN, TNT, and TATB are -21.6, -10.1, -74, and -55.8% respectively.

4 Conclusion

The onset temperature of HNX is similar to that of other trinitromethyl containing explosives such as 2-trinitromethylpyridine (114 °C), 2,6-bis(trinitromethyl)-pyridine (101 °C),

and 2-cyano-6-(trinitromethyl)pyridine (106 °C) [6]. HNX has a detonation velocity between that of TNT and RDX and activation energy higher than any of the common explosives tested. However, the lower onset temperature and detonation velocity make HNX unsuitable for the replacement of RDX.

Acknowledgements

This research was supported in part by the Office of Naval Research and the Naval Research Laboratory.

References

- [1] D. J. Vanderah, A. T. Nielsen, R. A. Hollins, C. Baum, Tetranitroquinodimethane (TNQ)-electron-deficient prototype for a new series of organic solid-state materials, *Mat. Res. Soc. Symp. Proc.* **1990**, 173, 155–159.
- [2] G. M. Sheldrick, Crystal structure refinement with SHELXL, *Acta Crystallogr. Sect. C* **2015**, 71, 3–8.
- [3] J. H. Flynn, L. A. Wall, A Quick, Direct Method for the Determination of Activation Energy from Thermogravimetric Data, *Polymer Letters* **1966**, 4, 323–328.
- [4] J. Zsakó, J. Zsakó, Kinetic Analysis of Thermogravimetric Data XIV. Three Integral Methods and Their Computer Programs, *J. Therm. Anal.* **1980**, 19, 333–345.
- [5] *Cheetah 6.0 User's Manual*, LLNL-SM-416166, **2010**.
- [6] E. F. C. Byrd, B. M. Rice, Improved Prediction of Heats of Formation of Energetic Materials Using Quantum Mechanical Calculations, *J. Phys. Chem. A* **2006**, 110, 1005–1013.
- [7] C. R. Groom, I. J. Bruno, M. P. Lightfoot, S. C. Ward, The Cambridge Structural Database, *Acta Crystallogr.* **2016**, B72, 171–179.
- [8] H. Yan, X.-P. Guan, Thermal Studies of 2-Azido-1,1-dinitroethyl compounds and Trinitromethyl Compounds, *J. Energ. Mater.* **1997**, 15, 283–288.
- [9] T. B. Brill, K. J. James, Kinetics and Mechanisms of Thermal Decomposition of Nitroaromatic Explosives, *Chem. Rev.*, **1993**, 93, 2667–2692.
- [10] G. Krien, H. H. Licht, J. Zierath, Thermochemical Investigations of Nitramines, *Thermochim. Acta*, **1973**, 6, 465–472.
- [11] D. L. Ornellas, J. H. Carpenter, S. R. Gunn, Detonation Calorimeter and Results Obtained With Pentaerythritol Tetranitrate (PETN), *Rev. Sci. Instrum.*, **1966**, 37, 907–912.
- [12] P. E. Rouse, Jr., Enthalpies of Formation and Calculated Detonation Properties of Some Thermally Stable Explosives, *J. Chem. Eng. Data*, **1976**, 21, 16–20.

Manuscript received: November 26, 2019
Revised manuscript received: January 17, 2020
Version of record online: April 29, 2020